Journal of Innovations in Engineering Education
JIEE 2026, Vol. 9, Issue 1.

https://doi.org/10.3126/jiee.v9i1.79529

THAPATHALI CAMPUS
Institute of Engineering
Tribhuvan University

A co-simulation study of differential braking electronic stability control for vehicle lateral stability

Rohan Shrestha[a], Sanjog Silwal [a] and Debendra Bahadur Raut[a,*]

[a]*Department of Automobile and Mechanical Engineering, Thapathali Campus, Institute of Engineering, Tribhuvan University, Nepal*

ARTICLE INFO

Article history:

Received 8 December 2025
Revised in 1 February 2026
Accepted 3 February 2026

Keywords:

CarSim
Software-in-loop
Multibody dynamics
Stability
Co-simulation

Abstract

This paper focuses on the design and simulation of a non-linear electronic stability control (ESC) system using MATLAB/Simulink, and validated through co-simulation with CarSim multibody dynamics (MBD) software. The ESC controller was designed in MATLAB/Simulink using sliding mode control technique due to its robust behavior under non-linearities, uncertainties, and disturbances. The controller utilized differential braking in order to generate corrective yaw moment that improves the lateral stability of the vehicle. For simulation, a front wheel driven C-class hatchback was used. The controller was evaluated using the sine with dwell (SwD) and tight double lane change (TDLC) tests within CarSim. The SwD was evaluated using the FMVSS 126 ESC homologation standards and the results demonstrated a reduction in the yaw rate NRMSE from 1.094 to 0.118 and sideslip angle NRMSE from 5.811 to 0.271. The DLC test was performed at 120 kmph which also demonstrated significant improvement in lateral path tracking.

1. Introduction

1.1. Background

With the growing population, the number of private vehicles on the road is also increasing, leading to a greater need for enhanced vehicle safety. While modern vehicles are equipped with various safety features that reduce the severity of injuries, they do not necessarily prevent accidents. Features such as crumple zones, airbags, and seatbelts improve driver safety and are particularly effective in frontal collisions. However, they do not enhance the vehicle's overall accident-avoidance capability. Improving a vehicle's handling characteristics through advanced control systems can enhance driver safety and help reduce the likelihood of accidents. Consequently, more than 70% of the passenger vehicles produced globally in 2024 were equipped with ESC due to its effectiveness to maintain vehicle stability and passenger safety [1].

ESC can be defined as a system that enhances vehicle stability by modifying the vehicle brake torques independently to apply the correct yaw moment in the vehicle [2]. The ESC system uses sensors that measure steering angle, yaw rate, vehicle speed, lateral acceleration, brake and accelerator pedal position, etc. to control vehicle behavior. A microcontroller estimates the intended direction and ideal motion of the vehicle and compares it with the actual motion. When the difference between these motions exceeds a certain threshold, the controller generates control signals that are sent to actuators, which in turn apply corrective forces to the vehicle. These corrective forces can be applied via the steering system (active steering control), differential brakes, torque distribution, and engine control (throttle release, retarded ignition timing, etc.) [3].

During extreme steering conditions, there is a tendency of the vehicle to oversteer or understeer and lose control. This is primarily due to the lateral forces generated during these extreme steering conditions. The main objective of this paper is the design and analysis of an ESC system that reduces the effects of lateral forces when cornering, bringing the vehicle to a stable condition. This is achieved by first developing a mathematical model of the controller in MATLAB/Simulink. The controller is then imported into CarSim and the controller is evaluated through co-simulation.

*Corresponding author:
raut.debendra@tcioe.edu.np (D.B. Raut)

1.2. Literature review

N.X. Tuan et al. [4] studied the stability of a car's trajectory in linear motion to study the influence of lateral forces and velocity of the vehicle. MATLAB/Simulink was used for model-based analysis and study the vehicle dynamics, while the results indicated that increased vehicle speed and lateral forces can increase lateral displacement by over 200%, which indicated the need of effective stability control systems. While A. Lie et al. [5] studied the effectiveness of ESC using induced exposure method to estimate the exposure to crashes with or without ESC, where rear-end collisions on dry surfaces were taken as the baseline crash type as these collisions are not influenced by ESC. Their study showed that ESC reduced the overall injury crashes by approximately 16.7% and 21.6% for serious and fatal crashes with effectiveness rising to 56.3% on wet roads and 49.2% on icy surfaces.

Y. Papelis et al. [6] also examined the ESCs' effectiveness on a high-fidelity driving simulator using two vehicles integrated into the simulator's dynamic code. The used different scenarios of loss of control of vehicle and allowed 120 participants of different age and gender to test with and without ESC. The results concluded the presence of ESC improved the vehicle control among the participants.

C.A.A. Delgado et al. [7] designed an ESC system using 3-DOF bicycle model with PID controller for side-slip and yaw rate control and a fuzzy controller for vertical dynamics which produced a corrective restoring torque and was evaluated using Fishhook and Sine-with-Dwell (SwD) maneuvers which verified the improved vehicle safety. T. Ensbury et al. [8] developed an ESC with simple open-loop-yaw-rate controller while PD was used to calculate the required corrective braking action. Co-simulation in Dymola and Simulink demonstrated improved lateral stability, steering and yaw rate performance.

D. Lu et al. [9] developed a two-layer ESC algorithm based on tire force control. The upper layer used linear quadratic regulator (LQR) and PID with feedforward in the lower layer. The method was validated via co-simulation and HiL tests under DLC and SwD tests/maneuvers at different speed and surface conditions which showed improved stability and control efficiency, especially on low-adherence surfaces, as compared to conventional PID-based methods.

Elmarakbi et al. [10] utilized a validated non-linear 6 DOF vehicle model and developed a fuzzy-logic integrated controller to supervise the coordination between standalone controllers. The controller integrated ESC with sliding surface control to control yaw torque, active suspension with PID and fuzzy logic controller to minimize load transfer between wheels, variable torque distribution with PI to control the drive torque in wheels and active front steering with PID and fuzzy to control the steer. This integrated setup showed improved response in both linear and non-linear handling regions.

H. Huang et al. [11] designed a full vehicle model, and conducted simulations to analyze the lateral acceleration, yaw rate, roll rate and steering wheel angle during constant-radius cornering maneuvers. The steady-state cornering performance at various speeds was evaluated and experiments were conducted to evaluate the effects of cornering stiffness, initial toe angle and initial camber angle on vehicle handling performance which showed that increasing cornering stiffness and initial toe angle improves the handling performance.

Jin et al. [12] applied a β phase plane approach with fuzzy-logic controller which uses side-slip angle deviation and yaw rate deviation for Electronic Stability Program (ESP) with 8DOF dynamic vehicle model and 2DOF model to compute yaw rate and sideslip angle with GIM tyre model to evaluate the performance of vehicle stability on low-adhesion surfaces in MATLAB/Simulink to determine the additional rear wheel steering and yaw moment. The results showed vehicle with ESP significantly reduced yaw rate and sideslip fluctuations, achieving quicker stabilization and better control as compared to vehicle without ESP.

Wang et al. [13] studied ESP control algorithm using electronic mechanical braking (EMB) and used ADAMS/Flex to improve the braking performance and safety. A coupled, rigid and flexible EMB system was generated in Ansys, while dynamics simulation was performed in AMESim, CarSim and MATLAB/Simulink which validated its effectiveness in improving the braking performance, vehicle stability and improved motor rotation. H. Li et al. [14] developed a ESP integrating ABS and TCS using Field-Programmable Gate Array (FPGA) to improve the vehicle stability. A 2DOF vehicle model was use, while sensors provided real-time data to enable ESP for adaptive braking control. The simulations concluded that ESP responded in less than 200ms, confirming the efficiency and vehicle stability.

S. Sivasubramanian et al. [15] developed a hybrid ESC with traction control system employing robust vehicle control model with a two-mode braking system (normal and smart modes) to enhance the wheel slip during slippery conditions and enhance the stability which demonstrated improved stability, anti-skid braking and improved traction control during extreme handling maneuvers or road conditions.

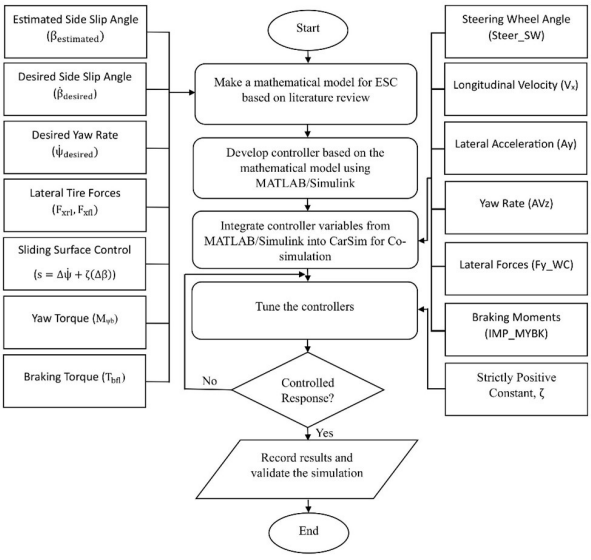

Figure 1: Flow chart of research methodology

2. Research methodology

This paper involves the design and analysis of ESC using MATLAB/Simulink. The controller is setup for co-simulation with a vehicle model (C Class, Hatchback 2017 shown in Figure 2) from CarSim, as it provides comprehensive and flexible environments and detailed vehicle systems/dynamics built into a single software to evaluate the performance of vehicle under different driving scenarios. Figure 1 shows the overall methodology.

2.1. Software used

The ESC controller is designed and implemented in MATLAB/Simulink R2023a and the developed controller is integrated with a vehicle model from CarSim 2017 to perform co-simulation and validate controller's performance.

2.2. Vehicle model and assumptions

The simulation-based testing requires a controller model and a vehicle model. ESC controller utilizes differential braking to achieve yaw stability. CarSim includes a full non-linear vehicle model using commercial multibody dynamic (MBD) software [16], which represents a real-world vehicle.

The vehicle model developed on MATLAB/Simulink is based on 7DOF which includes: longitudinal velocity, lateral velocity, yaw rate, and rotational velocities in the four wheels, while the CarSim has full non-linear 6DOF model. Some key assumptions were made while developing the vehicle model. The steering angle was assumed small to ignore the sine terms to determine the yaw torque. The linear tyre behavior was assumed to calculate the slip angles and desired yaw rate. The ratio of brake torque between front and rear wheels are fixed. The cornering stiffness was taken equal for both front and rear wheels. The brake pressure in each wheel is either zero or positive.

2.2.1. Model properties and geometry

The main parameters/properties used for the controller design are listed in Table 1. Most of these vehicle parameters are available in the CarSim whereas few of the parameters are assumed as such parameters that need to be obtained from multiple testing at well-facilitated testing laboratories.

Table 1: Vehicle parameters from CarSim (C Class, Hatchback 2017)[17]

Parameters	Symbol	Value
Mass of vehicle	m	1270 kg
Distance from CG to front axle	l_f	1015 mm
Distance from CG to rear axle	l_r	1895 mm
Track width	l_w	1916 mm
Distance from ground to CG	h	315 mm
Roll moment of inertia	I_{xx}	536.6 kg m^2
Yaw moment of inertia	I_{zz}	1536.6 kg m^2
Effective rolling radius of wheel	R_w	325 mm
Cornering stiffness of front wheels	C_f	40000 N/rad
Cornering stiffness of rear wheels	C_r	40000 N/rad

2.3. Estimated vehicle parameters

2.3.1. Side slip angle

In [18] a 7DOF model has been used to evaluate the lateral dynamics of the vehicle. The inertial acceleration

Figure 2: CarSim vehicle 3D model (C Class, Hatchback 2017)[17]

of the vehicle along the y-axis with reference to center of gravity is given by the following equation:

$$a_y = \ddot{y} + V_x\dot{\psi} \tag{1}$$

By rearranging equation 1 and substituting $\ddot{y} = \dot{\beta}V_x$, vehicle side slip velocity is calculated as follows:

$$\dot{\beta} = \frac{a_y}{V_x} - \dot{\psi} \tag{2}$$

Now integrating this equation with respect to time, we can estimate the value of side slip angle as follows:

$$\beta_{\text{estimated}} = \int \dot{\beta}\, dt \tag{3}$$

2.3.2. *Desired yaw rate and desired side slip angle*

Yaw rate is the rate of change of angle of vehicle with reference to the vertical axis. The desired yaw rate can be determined as [18]:

$$\dot{\psi}_{\text{des}} = \frac{V_x}{(l_f + l_r) + K_u V_x^2}\,\delta_{\text{wheel}} \tag{4}$$

K_u is the understeer coefficient which is calculated using the following equation,

$$K_u = \frac{m(l_r C_r - l_f C_f)}{2LC_f C_r} \tag{5}$$

The expression for the desired side slip angle in terms of vehicle parameters, longitudinal velocity and cornering stiffness is described in [18] as follows:

$$\beta_{\text{des}} = \frac{l_r - \dfrac{l_f m V_x^2}{2C_r(l_f + l_r)}}{(l_f + l_r) + K_u V_x^2}\,\delta_{\text{wheel}} \tag{6}$$

2.3.3. *Controller design*

The sliding surface controller is used for the controller design due to it robustness even with modelling errors and external disturbances. The control law is represented by the equation below, as described in [18]:

$$\begin{aligned}\frac{\rho + \cos\delta}{I_z} M_{\psi b} &= \frac{l_r}{I_z}(F_{yrl} + F_{yrr}) \\ &\quad - \frac{l_f}{I_z}(F_{yfl} + F_{yfr})\cos\delta \\ &\quad - u + \ddot{\psi}_{\text{target}} - \zeta(\dot{\beta} - \dot{\beta}_{\text{target}})\end{aligned} \tag{7}$$

The control law described in equation 7 requires slip angle, slip angle derivative, and front and rear lateral tire forces as inputs to produce a control signal in the form of yaw moment, $M_{\psi b}$. The slip angle and its derivatives are estimated using above equations, but the lateral tires forces are imported directly from CarSim itself as it provides a significantly improved tire force estimation and avoids the use of complex tire models within MATLAB/Simulink. The following sliding surface is suggested for this controller in [18]:

$$s = \dot{\psi} - \dot{\psi}_{\text{target}} + \zeta(\beta - \beta_{\text{target}}) \tag{8}$$

The control law enforcing switches across the surface is defined as [19]:

$$u = -\eta\,.\text{sign}(s) \tag{9}$$

where, η is the switching gain, u denotes the control input. This discontinuous law guarantees convergence to the sliding surface but may introduce chattering in practice. The $sign(s)$ is given by [19]

$$\text{sign}(s) = \begin{cases} +1, & s > 0 \\ 0, & s = 0 \\ -1, & s < 0 \end{cases} \tag{10}$$

2.3.4. *Chattering phenomenon and mitigation*

The discontinuous $sign(s)$ function in the sliding surface control results in high frequency oscillations known as chattering. These oscillations reduce actuator lifespan and reduces controller stability. To suppress chattering, the discontinuous switching function is replaced with a saturation function inside a boundary layer of thickness ϕ which smooths control action near the sliding surface while preserving robustness. The resulting equations is as follows:

$$\text{sat}\left(\frac{s}{\phi}\right) = \begin{cases} \dfrac{s}{\phi}, & |s| < \phi \\ \text{sign}(s), & |s| \geq \phi \end{cases} \tag{11}$$

Thus, the modified control law becomes:

$$u = -\eta\,.\text{sat}\left(\frac{s}{\phi}\right) \tag{12}$$

2.3.5. *Tuning parameter sweep*

In order to tune the parameters ζ, η, and ϕ, a systematic parameter sweep was performed. The values of ζ and η were varied across a practical range to enforce reachability, while the value of ϕ was adjusted to minimize chattering. Each parameter set was tested under double lane change (DLC) maneuvers at 120 km/h with a road friction coefficient $\mu = 0.85$. The observed performance metrics were the RMSE of yaw rate and lateral path deviation.

2.3.6. *Stability tests*

To rigorously evaluate the controller robustness under high-speed maneuvers, three complementary stability tests were applied. Each test targets a distinct dimension of stability, ensuring that claims are substantiated across Lyapunov, time-domain, and oscillatory perspectives.

1. **Lyapunov sign test**

   The Lyapunov sign test verifies reachability of the sliding surface. The Lyapunov derivative is defined as:

   $$q = s \times \dot{s} \tag{13}$$

   Where s is the sliding surface and $\dot{s}$ is its derivative. The system's stability is considered positive if the derivative q is negative for a majority of the time, which indicates that the system is converging to the sliding surface. For the controller to pass, at least 70% of samples have to yield a negative q, and the mean q has to be negative. This criterion follows Lyapunov's second method, where the sign of the derivative determines stability [20].

2. **Time-domain boundedness**

   This test evaluates whether critical vehicle status remains within safe limits during aggressive maneuvers (DLC). The boundedness criteria are the normalized root-mean-square errors (NRMSE) for yaw rate and lateral path deviations.

   $$\text{NRMSE} = \frac{1}{r_{\text{peak}}} \sqrt{\frac{1}{n} \sum_{i=1}^{n} (r_i - \bar{r}_i)^2} \tag{14}$$

   Where, r_{peak} is the peak value of target value, r_i is the measured value and $\bar{r}_i$ is target value. The test is carried out at 120 km/h at $\mu = 0.85$, with $\pm 10\%$ variation in speed and friction. This formulation follows established boundedness criteria for ESC evaluation in vehicle dynamics [18].

3. **Limit cycle detection**

   This test ensures that the closed loop system does not exhibit sustained oscillations or self excited limit cycles during aggressive maneuvers. Limit cycles represent undesirable nonlinear behavior where oscillations persist even without external excitation, undermining controller stability. Three checks are performed for this test.

   a) **Envelope decay**

   Oscillation amplitude must decrease over time.

   b) **Power Spectral Density (PSD) peak ratio**

   $$\text{PeakRatio} = \frac{\max(P(f))}{\text{median}(P(f))} \leq 5 \tag{15}$$

   Where $P(f)$ is the PSD of the sliding variable or yaw rate.

   c) **Autocorrelation tail**

   $$\max\left(R_{ss}(\tau)\right) < 0.2 \tag{16}$$

   Where $R_{ss}()$ is the autocorrelation of the sliding variable. A low tail value indicates that oscillations decay rather than persist over time.

   These criteria follow established practices in nonlinear control and vehicle dynamics for detecting and preventing limit cycles [21].

2.3.7. *Differential braking*

The yaw torque from differential braking is calculated to be [18]:

$$M_{\psi b} = \frac{l_w}{2}(F_{xfr} - F_{xfl}) = \frac{l_w}{2}\Delta F_{xf} \tag{17}$$

The desired brake pressure at front left and right wheels are determined as [18]:

$$P_{bfr} = P_0 + (1 - a)\frac{\Delta F_{xf} R_w}{A_w \mu_b R_b} \tag{18}$$

$$P_{bfl} = P_0 - a\frac{\Delta F_{xf} R_w}{A_w \mu_b R_b} \tag{19}$$

Here, R_b is the brake radius, A_w is the area of wheel brake, μ_b is the coefficient of friction of brake.

[18] suggests choosing the constant a such that applied brake pressures are always positive and $0 \leq a \leq 1$. The

term P_0 denotes the initial brake pressure that is applied by the driver. The selection of a depends on whether the driver is applying brakes or not. For the purpose of this controller, it is assumed that the driver is never applying the brakes, $P_0 = 0$. The braking torque for any wheel is given by [18]:

$$T_b = A_w \mu_b R_b P_b \tag{20}$$

Now combing equations 17, 18 and 20, and assuming $a = 0$, we get the following equation for braking torque on right wheel.

$$T = \frac{2\Delta M_{\psi b} R_w}{l_w} \tag{21}$$

The braking torque on the left wheel will be zero, creating a differential braking effect. A similar equation can be obtained for left wheel braking torque using equation [19].

3. Simulation

Co-simulation is performed between Differential Braking ESC in Simulink and CarSim. The link between CarSim and Simulink is created by the 'CarSim S-Function'. When the simulation is run, the S-Function block communicates with the CarSim VS Solver library to transfer the data for co-simulation.

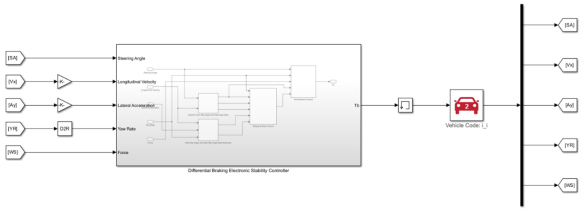

Figure 3: Simulink block setup for electronic stability control for co-simulation

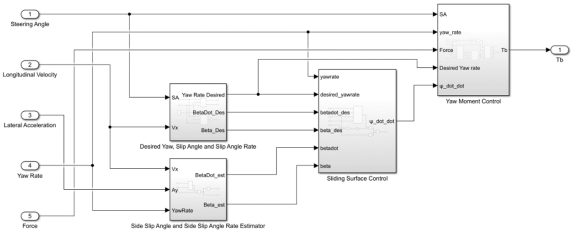

Figure 4: Structure of differential braking electronic stability controller

The s-function block exports various variables to MATLAB which include steering wheel angle, longitudinal velocity, lateral acceleration, yaw rate, lateral forces of each wheel and X-Y coordinates of vehicle origin. These variables need to be selected within the CarSim interface to export them via CarSim's Export Channel. The S-function block also imports the calculated brake torques for each wheel from the MATLAB controller for controlling the vehicle's lateral motion. The braking data for each wheel needs to be individually assigned in the CarSim interface when importing the data from the controller via CarSim's Import Channels.

4. Results and discussion

4.1. Tuning parameters

Table 2: Comparison of NRMSE values for tuning of ζ, η and ϕ

ζ	NRMSE yaw rate	NRMSE path
0.1	0.414	0.510
0.2	0.414	0.472
0.3	0.414	0.470
0.4	0.413	0.468
0.5	0.410	0.466
0.6	0.408	0.465
0.7	0.408	0.464
0.8	0.415	0.463
0.9	0.422	0.463
1.0	0.430	0.465
η	**NRMSE yaw rate**	**NRMSE path**
1	0.335	0.364
2	0.351	0.366
3	0.376	0.369
4	0.376	0.368
5	0.387	0.375
6	0.388	0.376
7	0.294	0.329
8	0.314	0.336
9	0.340	0.341
10	0.378	0.377
ϕ	**NRMSE yaw rate**	**NRMSE path**
0.1	0.232	0.321
0.2	0.220	0.318
0.3	0.204	0.318
0.4	0.200	0.321
0.5	0.194	0.319
0.6	0.188	0.319
0.7	0.186	0.319
0.8	0.184	0.319
0.9	0.184	0.319
1.0	0.183	0.320

The parameter sweep conducted for ζ, η and ϕ provided clear evidence of their influence on controller performance. The η and ϕ values were fixed at 10 and 0.5 for

the ζ sweep. The ζ value was varied between 0.1 and 1. The parameter sweep showed that ζ value 0.7 had the lowest combined NRMSE yaw rate and path deviation values. The ζ value was then fixed at 0.7 to perform the other sweeps. In case of η, the parameter sweeps from 1 to 10 highlighted $\eta = 7$ as the most effective choice, yielding lowest yaw and path deviation error. For the final sweep, ζ was fixed at 0.7 and η was fixed at 7. NMRSE analysis of ϕ values showed that the higher ϕ values give lower yaw errors. However, higher ϕ values can result in increased chattering in control action. To avoid excessive switching while maintaining low error, ϕ value 0.3 was selected as compromise. The selected values are $\zeta = 0.7$, $\eta = 7$, $\phi = 0.3$.

4.2. Stability test with tuned parameters

Following the parameter sweep and optimal selection, the stability tests were applied using the tuned controller values. The results for the three stability criteria are summarized below.

Test 1: Lyapunov sign criterion

Table 3: Results of the Lyapunov sign test at $\eta = 5$ and 7

η	q_{mean}	$q\%$
5	-0.00071	60.3%
7	0.00252	64.8%

The Lyapunov sign test revealed some issues with the selected η values. At $\eta = 7$, the Lyapunov results showed a mean $q = +0.00252$ with 64.8% negative samples, indicating marginal stability in certain segments. In contrast, at $\eta = 5$, the mean q shifted to -0.00071, with 60% of the samples satisfying the negative condition. Although the NRMSE values at $\eta = 5$ were slightly higher, the negative mean q confirmed asymptotic stability and stronger convergence to the sliding surface. Ultimately, $\eta = 5$ was chosen as the tuned parameter, prioritizing stability and robustness.

Test 2: Time-domain boundedness

The tuned parameters were evaluated against the normalized RMSE thresholds for yaw rate and path deviation. For robustness evaluation, a degradation of up to 15% in NRMSE relative to nominal conditions is considered acceptable. The nominal condition for the test is TDLC at 120 km/h with $\mu = 0.85$. The NRMSE yaw rate and NRMSE path deviation obtained at the nominal conditions were 0.314 and 0.336 respectively. Therefore, the maximum allowable NRMSE errors with a 15% margin were 0.361 and 0.386 for yaw rate and path deviation respectively.

All tested variations remained within the allowable bounds, confirming that the tuned controller maintains robust tracking performance under speed and friction changes.

Test 3: Limit-cycle detection

Segment-wise limit-cycle detection confirmed that, under most conditions, the envelope decay remained monotonic, PSD peak ratios were below the threshold of 5, and autocorrelation tails decayed rapidly (< 0.2). A single failure was observed in the mid-segment at $\mu = 0.75$, where the envelope decay was non-monotonic, indicating a tendency toward sustained oscillations. Overall, the tuned controller demonstrated robust avoidance of limit cycles across speed variations with sensitivity to reduced friction conditions.

4.3. Slowly Increasing Steer (SIS) procedure

The ESC controller is evaluated using the sine-with-dwell (SwD) and double lane change (DLC) tests. The DLC test is used to assess the robustness of the system and the lateral tracking capability of the vehicle. The SwD test is performed according to the performance requirements established by FMVSS 126 and UN/ECE-R 13H.

To perform the SwD test, the steering angle A must first be determined. The slowly increasingsteer (SIS) procedure is used to determine A, following the specifications in UN/ECE-R 13H.The test is conducted at a constant vehicle speed of 80 km/h with an allowable deviation of ± 2 km/h. The steering angle is increased at a rate of 13.5°/s. The procedure continues until a lateral acceleration of approximately 0.5 g is reached. The steering angle A is defined as the angle at which a lateral acceleration of 0.3 g is produced [22].

From Figure. 5, the lateral acceleration of the vehicle reaches 0.3 g at 2.061 s, and the corresponding steering amplitude A at that instant is 27.81°. For the simulation tests, steering amplitude of $6.5A$ is chosen as it represents extreme driving conditions. The steering angle is calculated to be $6.5A = 180.765°$. Since the value of $6.5A$ is calculated to be less than 270°, the final value for steering angle is taken as 270° as per the specifications in UN/ECE-R 13H.

4.4. Sine with Dwell (SwD) test

The steering input consists of a $0.7Hz$ sine wave followed by a dwell phase where angle is held before returning to zero, as specified in FMVSS 126.

With ESC, yaw rate tracked the steering input with minimal lag and oscillations were quickly damped. Without

Table 4: Time-domain boundedness results under 10% variations in speed and friction

Condition	Speed/μ	NRMSE yaw rate	NRMSE path deviation	Verdict
-10% Speed	110, 0.85	0.331	0.322	Pass
$+10\%$ Speed	130, 0.85	0.318	0.298	Pass
-10% μ	120, 0.75	0.358	0.377	Pass
$+10\%$ μ	120, 0.95	0.300	0.301	Pass

Table 5: Limit-cycle detection results under 10% variations in speed and friction

Condition	Speed/μ	Entry (ED/PSD/AC)	Mid (ED/PSD/AC)	Exit (ED/PSD/AC)	Verdict
		Monotonic	Monotonic	Monotonic	
-10% Speed	110, 0.85	1.00	1.17	1.43	Pass
		0.195	0.162	0.134	
		Monotonic	Monotonic	Monotonic	
$+10\%$ Speed	130, 0.85	1.00	1.17	1.45	Pass
		0.184	0.167	0.113	
		Monotonic	Non-Monotonic	Monotonic	
-10% μ	120, 0.75	1.00	1.08	1.42	Fail
		0.182	0.172	0.140	
		Monotonic	Monotonic	Monotonic	
$+10\%$ μ	120, 0.95	1.00	1.14	1.42	Pass
		0.184	0.186	0.121	

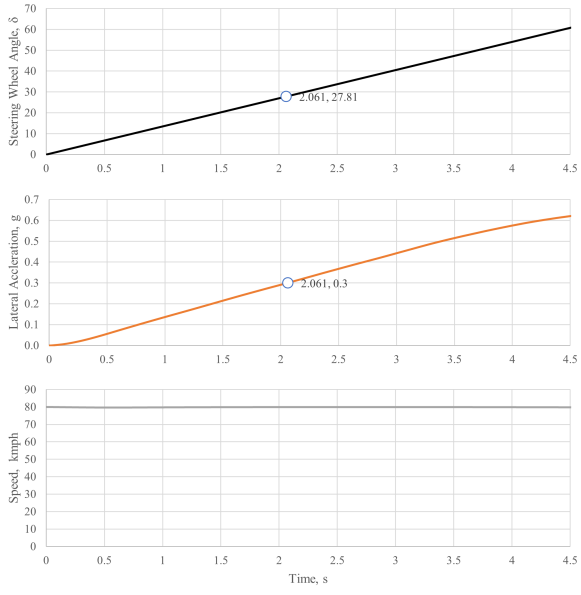

Figure 5: Graphs of lateral acceleration, steering wheel angle and speed obtained after SIS maneuver at 80kmph

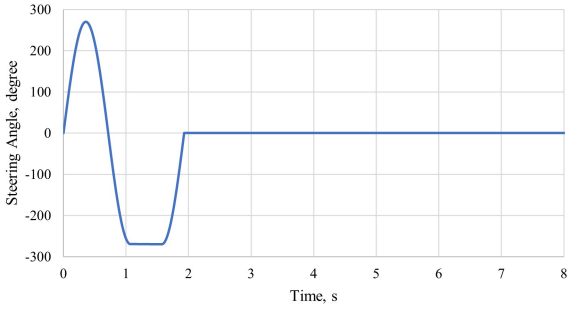

Figure 6: Steering angle input for the Sine with Dwell test

ESC, oscillations persisted and recovery was delayed.

The SwD test demonstrated that ESC reduced yaw rate NRMSE from 1.094 to 0.118 and sideslip angle NRMSE from 5.811 to 0.271. This reduction in NRMSE highlights the controller's ability to suppress instability and maintain trajectory fidelity under aggressive steering inputs which can be explained from fundamental vehicle stability principles. The yaw rate infers the steering response of a vehicle to steering input, and high yaw rate indicates loss of control. Without ESC, high steering inputs can cause asymmetric tire force saturation leading to yaw oscillations and difficult recovery.

With ESC, differential braking generates a corrective yaw moment which opposes the deviation between actual and desired yaw rate increases yaw damping of the vehicle and maintains wheel rpms, which results in controlled yaw rate and stable vehicle in lateral motion. The reduction in sideslip angle shows improved lateral tire forces and prevention of tire saturation required for

Table 6: NRMSE values of yaw rate and sideslip angle during SwD test with and without ESC

ESC	NRMSE Yaw Rate	NRMSE Vehicle Sideslip Angle
Not Equipped	1.094	5.811
Equipped	0.118	0.271

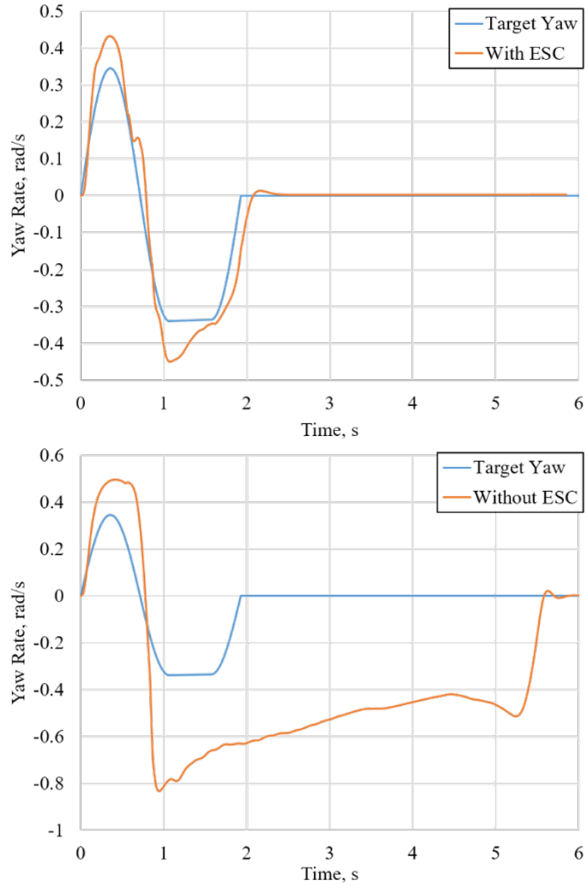

Figure 7: Comparison of the yaw rate with and without the ESC equipped for the Sine with Dwell test

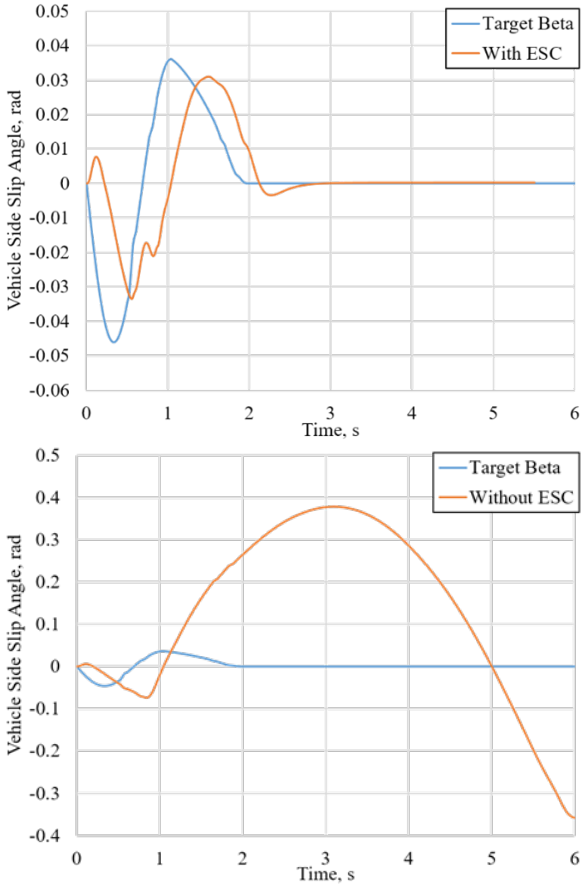

Figure 8: Comparison of vehicle side slip angle with and without the ESC equipped for the Sine with Dwell test

maintaining lateral stability.

Sideslip angle is a critical indicator for lateral stability, as high sideslip angle indicates loss of linear tyre behavior and increased risk of vehicle spin. Without ESC, it grew unbounded, indicating that the vehicle operated beyond the stable region.

While sideslip angle remained bounded with ESC throughout the maneuver. Although it is not controlled directly, the regulation of yaw rate via differential braking indirectly maintains the sideslip angle by stabilizing vehicle rotation. This sideslip angle behavior confirms that the proposed controller generates lateral force at the tyres which enhances vehicle stability under aggressive lateral motion.

With ESC, lateral acceleration closely followed the steering input indicating controlled response. Without ESC, the vehicle exhibited excessive lateral acceleration and drift, consistent with unstable behavior. This confirms that ESC effectively regulates lateral dynamics and maintains trajectory under the SwD maneuver.

The vehicle completes steering at 1.93 s. The vehicle without the ESC equipped exhibited a peak yaw rate $-0.83\,\mathrm{rad/s}$ ($-47.79°/\mathrm{s}$), with values remaining high at $t_0 + 1.00\,\mathrm{s}$ ($-0.54\,\mathrm{rad/s}$, $-31.38°/\mathrm{s}$) and $t_0 + 1.75\,\mathrm{s}$ ($-0.48\,\mathrm{rad/s}$, $-27.62°/\mathrm{s}$). The yaw rate deviates from the zero until approximately 5.7 s, indicating prolonged instability.

Table 7: Results of the Sine with Dwell test

ESC	δ [°]	$\dot{\psi}_{\text{Peak}}$ [°/s]	$\dot{\psi}_{(t_0+1.00)}$ [°/s]	$\dot{\psi}_{(t_0+1.75)}$ [°/s]	$Y_{1.07}$ [m]
Not Equipped	270	-47.79	-31.38	-27.62	4.25
Equipped	270	-25.79	0.144	0.153	2.56

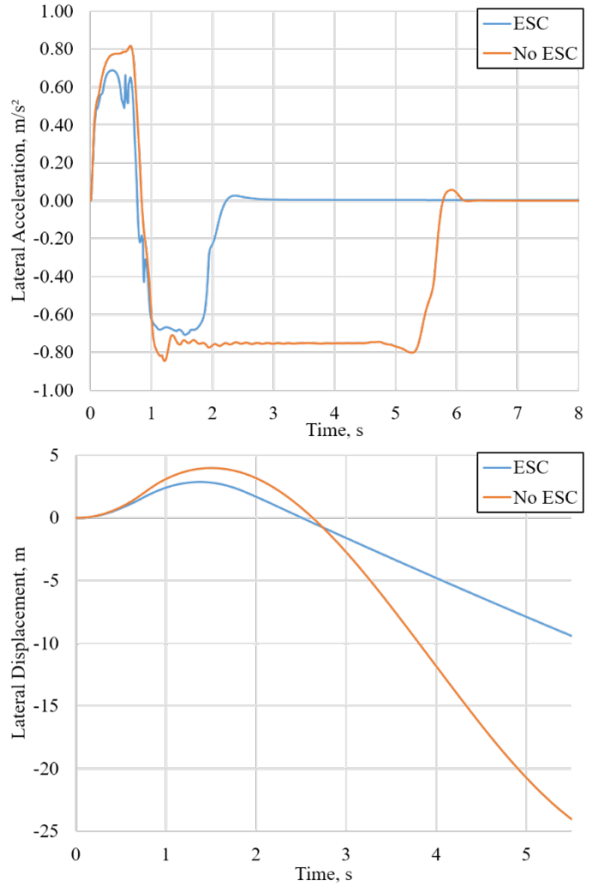

Figure 9: Comparison of the lateral acceleration and lateral displacement with and without the ESC equipped for the Sine with Dwell test

With the ESC equipped, the peak yaw rate is reduced to $-0.45\,\text{rad/s}$ ($-25.78°/\text{s}$), and yaw rate values are observed to be $0.00252\,\text{rad/s}$ ($0.144°/\text{s}$) and $0.00267\,\text{rad/s}$ ($0.153°/\text{s}$) at $t_0 + 1.00\,\text{s}$ and $t_0 + 1.75\,\text{s}$ respectively. Yaw rate returned to stability within 2.1 s. The results confirmed that with the ESC equipped, the yaw oscillations were rapidly suppressed.

The uncontrolled vehicle achieved yaw percentages of 65.66% and 57.79% which exceeds the yaw percentage thresholds of 35% and 20%, failing the stability criteria. The lateral displacement value of 4.25*m* met the responsiveness criteria. In contrast, the ESC equipped vehicle achieved yaw percentages of 0.558% and 0.593% and a lateral displacement of 2.56*m*, satisfying both stability and responsiveness requirements. The improvements seen in SwD test are achieved via selective application of differential braking which applies braking torque to individual wheels which generates a yaw moment which counteracts undesired vehicle rotation without additional steering. The applied differential braking is transient and asymmetrical, activating only when the yaw deviation exceeds the stability thresholds.

Table 8: FMVSS 126 yaw rate percentage criteria comparison for Sine with Dwell test

ESC	$\frac{\dot{\psi}_{(t_0+1.00)}}{\dot{\psi}_{\text{Peak}}}$ [%]	$\frac{\dot{\psi}_{(t_0+1.75)}}{\dot{\psi}_{\text{Peak}}}$ [%]
Not Equipped	65.66	57.79
Equipped	0.558	0.593

These results highlight the controller's ability to reduce yaw oscillations by an order of magnitude and restore stability significantly faster than the baseline. The ESC not only meets the FMVSS 126 compliance but also demonstrates enhanced trajectory tracking under aggressive steering inputs.

4.5. Tight Double Lane Change

The ISO 3888-2 standard describes the tight double-lane change maneuver, which tests the ability of the vehicle to avoid obstacles while driving in extreme condition. In this test, the driver initially accelerates the vehicle to a certain predefined velocity. Once the velocity is reached, the throttle input is held constant throughout the maneuver. The driver then steers the vehicle to follow a designated path into the left lane, simulating quick and sharp obstacle avoidance. The TDLC maneuver is completed, when the vehicle is steered immediately back to the initial lane [23]. A speed of 120 km/h was chosen for TDLC maneuver which is typically higher than ISO 3888-2 speeds, as in this speed there is significantly increased lateral forces and yaw instability allowing a precise assessment of controller robustness and safety margins.

During the high-speed TDLC test, it is observed that the vehicle tends to deviate from the required path in the absence of the ESC. This is primarily caused due to the lateral instability of the vehicle that occurs due extreme

Table 9: Comparison of results of Tight Double Lane Change test between the proposed system and Jung (2020) [16]

Parameters	Our Study	Jung (2020)
Average Longitudinal Velocity ($V_{x,\text{avg}}$)	118.7	111.58
Maximum Lateral Acceleration ($a_{y,\text{max}}$)	0.707 g	0.791 g

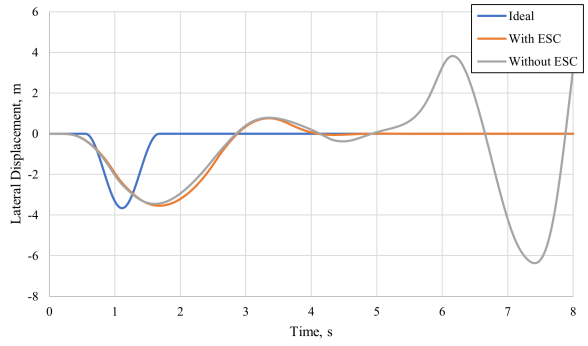

Figure 10: Plot showing the lateral displacement with respect to time for the tight double lane change maneuver at 120 km/h

steering input that is required to carry out the TDLC test. This instability is also amplified by the high speeds at which the test is conducted. When the test is carried out at lower speeds, the instability is significantly lower and the vehicle is able to return to its intended path. However, with the integration of the ESC, the vehicle is able to improve its lateral stability and return to its tracked path. The ESC utilizes differential braking, which means that braking at each of the four wheels is individually controlled to create a corrective yaw moment.

To evaluate the effectiveness of the proposed controller, a benchmarking comparison was conducted between the vehicle with the ESC equipped and a baseline vehicle without the ESC equipped. The baseline vehicle represents the response of the vehicle governed wholly by the tire and chassis dynamics with no braking based yaw intervention or stability control. The comparison indicates that the ESC designed in this paper achieved substantially lower yaw rate and sideslip errors. With the ESC equipped there was significantly faster stability recovery as well as reduced lateral displacement. These improvements demonstrate a substantial improvements to vehicle stability relative to the baseline configuration.

The results were compared with those reported in [16], where a similar ESC system was implemented using Direct Yaw Control (DYC) and Active Front Steering (AFS).

During the TDLC tests, the average longitudinal velocity was 118.7 km/h for the proposed system and 111.58 km/h in [16], while the maximum lateral acceleration recorded was slightly lower at 0.707 g compared to 0.791 g in [16]. The simulation results indicate that the vehicle returned to its original lane within 5 seconds without losing stability. In the absence of ESC, the lateral deviation increased significantly, making path tracking difficult. Furthermore, the DYC system in [16] showed greater lateral deviation during lane realignment. These observations suggest that the proposed ESC design improves both vehicles tracking performance and lateral stability during high-speed maneuvers.

Unlike the controller presented in [16] which employs Active Front Steering and Direct Yaw Control, the proposed controller utilizes only differential braking to generate corrective yaw moments. Despite utilizing fewer controllers, the proposed controller produces comparable lateral stability and path recovery results under Sine with Dwell and high speed-speed TDLC conditions. This highlights the robustness and effectiveness of the sliding mode based braking controller under nonlinear operating conditions.

5. Conclusion

Although the mathematical model for the controller is based on the Vehicle Dynamics and Control by Rajesh Rajamani, the novelty of this research lies in the design, co-simulation and stability validation of a nonlinear ESC with emphasis on robustness assessment under extreme driving conditions. A distinguishing feature of this paper is the validation of ESC performance under ISO 3888-2 TDLC, rarely employed for ESC validation, due to higher yaw rate and reduced lateral acceleration margins requirement in comparison to conventional DLC maneuvers. Motivated by this gap, this paper also highlights the application of multi-criteria stability validation combining Lyapunov sign analysis, time-domain boundedness and limit-cycle detection for better evaluation of ESC.

Across all tests, the controller consistently demonstrated improved stability compared to baseline vehicle without ESC. The proposed controller demonstrates significant reduction in yaw rate and sideslip angles by using differential brakes. Lyapunov analysis confirmed bounded convergence, boundedness highlighted sensitivity un-

der reduced friction, and limit cycle checks showed monotonic decay with only one marginal case. Most notably, the Sine with Dwell benchmark revealed order of magnitude reductions in yaw rate and sideslip NRMSE, validating the controller's ability to suppress instability and maintain trajectory fidelity.

Overall, the proposed ESC system enhances vehicle handling and stability under aggressive maneuvers. Future work will extend validation through Hardware in the Loop testing and comparative studies with advanced strategies such as LQR and MPC to further strengthen robustness and real world applicability.

6. Limitations and Future Work

i. Perform Hardware-in-Loop (HiL) test to access the system's performance on real-time system.

ii. Implement Active Front Steering (AFS) to further improve the vehicle stability.

iii. Implement Torque Vectoring method to precise control the torque output in each wheel.

Nomenclature

a	Brake pressure distribution factor (−)
a_y	Lateral acceleration (m/s^2)
A_w	Brake area of wheel (m^2)
C_f	Cornering stiffness for front tires (N/rad)
C_r	Cornering stiffness for rear tires (N/rad)
ΔF_{xf}	Extra differential longitudinal force (N)
F_{xfr}	Differential longitudinal tire force on front right (N)
F_{xfl}	Differential longitudinal tire force on front left (N)
F_{yfl}	Lateral tire force on front left (N)
F_{yfr}	Lateral tire force on front right (N)
F_{yrl}	Lateral tire force on rear left (N)
F_{yrr}	Lateral tire force on rear right (N)
I_{xx}	Roll moment of inertia (kg m^2)
I_{zz}	Yaw moment of inertia (kg m^2)
K_u	Understeer coefficient (−)
L	Vehicle wheelbase (m)
l_f	Distance from CG to front axle (m)
l_r	Distance from CG to rear axle (m)
l_w	Track width (m)
m	Vehicle mass (kg)
$M_{\psi b}$	Yaw torque for differential braking (Nm)
P_0	Initial brake pressure (MPa)
P_{bfl}	Brake pressure at front left wheel (MPa)
P_{bfr}	Brake pressure at front right wheel (MPa)
R_w	Effective rolling radius (m)
R_b	Brake radius (m)
s	Sliding surface (°/s)
$\dot{s}$	Derivative of sliding surface (°/s^2)
t_0	Time to completion of steer (s)
T_{bfl}	Drive torque on front left wheel (Nm)
T_{bfr}	Drive torque on front right wheel (Nm)
V_x	Longitudinal velocity (m/s)
$\ddot{y}$	Lateral acceleration in CG frame (m/s^2)
μ_b	Brake friction coefficient (−)
δ_{wheel}	Wheel steering angle (°)
δ	Steering angle (°)
ψ	Yaw angle (°)
$\dot{\psi}$	Yaw rate (°/s)
$\ddot{\psi}$	Yaw acceleration (°/s^2)
$\dot{\psi}_{\text{des}}$	Desired yaw rate (°/s)
$\dot{\psi}_{\text{target}}$	Target yaw rate (°/s)
$\dot{\psi}_t$	Yaw rate at time t (°/s)
$\dot{\psi}_{\text{peak}}$	Peak yaw rate from 0.7 Hz SwD input (°/s)
β	Side slip angle (°)
$\dot{\beta}$	Side slip velocity (°/s)
β_{des}	Desired side slip angle (°)
$\beta_{\text{estimated}}$	Estimated side slip angle (°)
ρ	Front–rear brake proportioning (−)
η	Sliding mode convergence gain (s^{-1})
ζ	Weighting factor in sliding surface (s^{-1})

References

[1] Electronic stability control (esc) market size, share, growth, and industry analysis[Z]. 2024.

[2] National Highway Traffic Safety Administration. Federal motor vehicle safety standard no. 126: Electronic stability control systems[Z]. 2007.

[3] Kinjawadekar B T S, Guenther D A, Heydinger A J G. Model-based design of electronic stability control system for passenger cars[Z].

[4] Nguyen T X, Bui H V. Study of the influence of lateral forces and velocity on the lateral dynamics of automobile[J/OL]. EUREKA: Physics and Engineering, 2024(2): 70-78. DOI: 10.21303/2461-4262.2024.003173.

[5] Lie A, Tingvall C, Krafft M, et al. The effectiveness of electronic stability control (esc) in reducing real life crashes and injuries[J/OL]. Traffic Injury Prevention, 2006, 7(1): 38-43. DOI: 10.1080/15389580500346838.

[6] Papelis Y E, Watson G S, Brown T L. An empirical study of the effectiveness of electronic stability control system in reducing loss of vehicle control[J/OL]. Accident Analysis and Prevention, 2010, 42(3): 929-934. DOI: 10.1016/j.aap.2009.04.018.

[7] Delgado C A A, Felix A A, Ripari G, et al. Vehicle stability using an automotive electronic system: Yaw rate, side-slip angle, and roll rate control[C/OL]// Proceedings of the 28th International Congress of Mechanical Engineering. 2025. DOI: 10.26678/ABCM.COBEM2023.COB2023-0498.

[8] Ensbury T, Horn N, Dempsey M. Dymola and simulink in co-simulation: A vehicle electronic stability control case study[Z].

[9] Lu D, Ma Y, Yin H, et al. Development and validation of electronic stability control system algorithm based on tire force observation[J/OL]. Applied Sciences, 2020, 10(23): 8741. DOI: 10.3390/app10238741.

[10] Elmarakbi A, Rengaraj C, Wheatley A, et al. The influence of electronic stability control, active suspension, driveline and front steering integrated system on the vehicle ride and handling[Z]. 2013.

[11] Huang H H, Tsai M J. Vehicle cornering performance evaluation and enhancement based on cae and experimental analyses[J/OL]. Applied Sciences, 2019, 9(24): 5428. DOI: 10.3390/app9245428.

[12] Jin L, et al. Study on electronic stability program control strategy based on the fuzzy logical and genetic optimization method[J/OL]. Advances in Mechanical Engineering, 2017, 9 (5). DOI: 10.1177/1687814017699351.

[13] Wang Z, Hong Z, Wang Y, et al. Study on vehicle electronic stability program control algorithm under electronic mechanical braking[J/OL]. Chemical Engineering Transactions, 2018, 66: 739-744. DOI: 10.3303/CET1866124.

[14] Li H, Du Y. Research on the vehicle esp system in fpga[C/OL]// Chinese Control and Decision Conference. 2010: 294-298. DOI: 10.1109/CCDC.2010.5499062.

[15] Sivasubramanian S, Basha N A, Ajai A R, et al. Electronic stability traction control system in vehicle[J/OL]. International Journal of Engineering Research & Technology, 2019, 7(06). DOI: 10.17577/IJERTCONV7IS06015.

[16] Jung W. Development of an electronic stability control for improved vehicle handling using co-simulation[Z]. 2020.

[17] Mechanical Simulation Corporation. Carsim vehicle dynamics simulation software – class c vehicle model[Z]. 2017.

[18] Rajamani R. Vehicle dynamics and control[M/OL]. Boston, MA: Springer, 2012. DOI: 10.1007/978-1-4614-1433-9.

[19] The MathWorks, Inc. Sliding mode control[EB/OL]. n.d.. https://www.mathworks.com/help/slcontrol/ug/design-sliding-mode-control-reaching-law.html.

[20] Tedrake R. Underactuated robotics: Lyapunov stability[EB/OL]. n.d. https://underactuated.mit.edu/lyapunov.html.

[21] Slotine J J E, Li W. Applied nonlinear control[M]. Taiwan: Prentice Hall, 2005.

[22] United Nations Economic Commission for Europe. Regulation no. 13-h: Uniform provisions concerning the approval of passenger cars with regard to braking[R/OL]. UNECE, 2015. http://data.europa.eu/eli/reg/2015/2364/oj.

[23] The MathWorks, Inc. Double-lane change maneuver[EB/OL]. n.d.. https://www.mathworks.com/help/vdynblks/ug/double-lane-change-maneuver.html.